Supplementary Information

Optimizing the active interface structure of MnO_2 to achieve sustainable water oxidation in Acidic Medium

Sanjiang Pan [1,2,3*#], Shenao Wang[1#], Yu Wang[1#], Hang Li[1], Deng Zhao[1], Yang Fu[4], Hua Liu[1], Jiajing Kou[1,2,3], Nan Li[1,3*], Desong Wang[2*]

[1] School of Vehicle and Energy, Yanshan University, Qinhuangdao 066004, China

[2] State Key Laboratory of Metastable Materials Science and Technology, Yanshan University, Qinhuangdao, 066004 China

[3] Hebei Engineering Research Center for Low Carbon Development and Resource Utilization of Fossil Energy Sources, Yanshan University, Qinhuangdao 066004, China

[4] Jiangmen Laboratory of Carbon Science and Technology, Jiangmen 529020, China

[*]E-mail: linan@ysu.edu.cn (N.L.), dswang06@126.com (D.W.), pansanjiang@ysu.edu.cn (S.P)

[#]These authors contributed equally

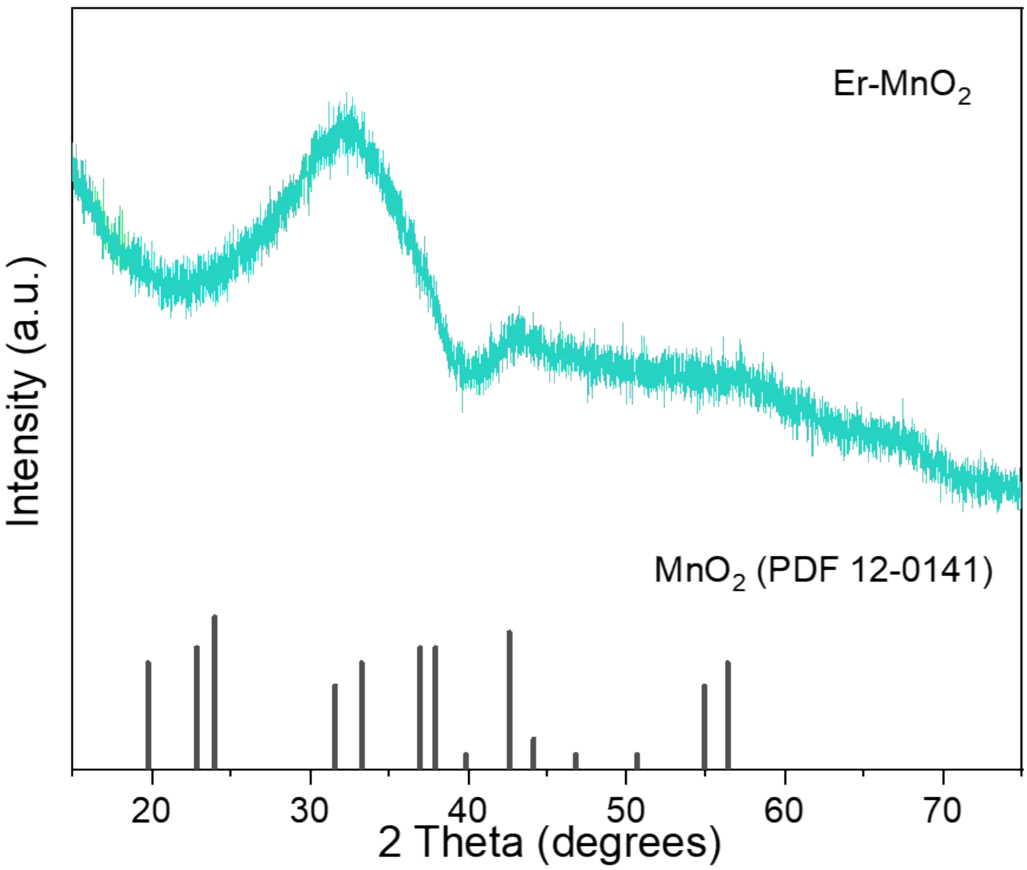

Supplementary Figure 1. XRD patterns of Er-MnO_2.

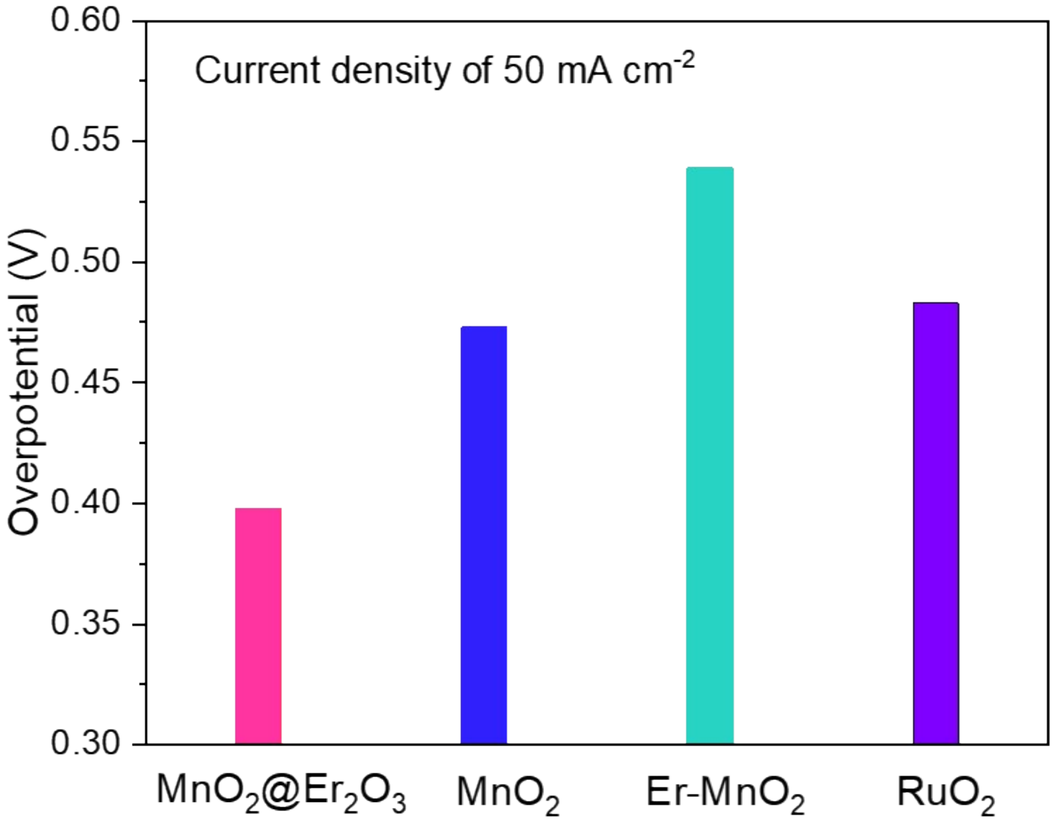

Supplementary Figure 2. The overpotential of oxygen evolution reaction with a current density of 50 mA cm^{-2} was compared in 0.5 M H_2SO_4 electrolyte with different electrocatalysts.

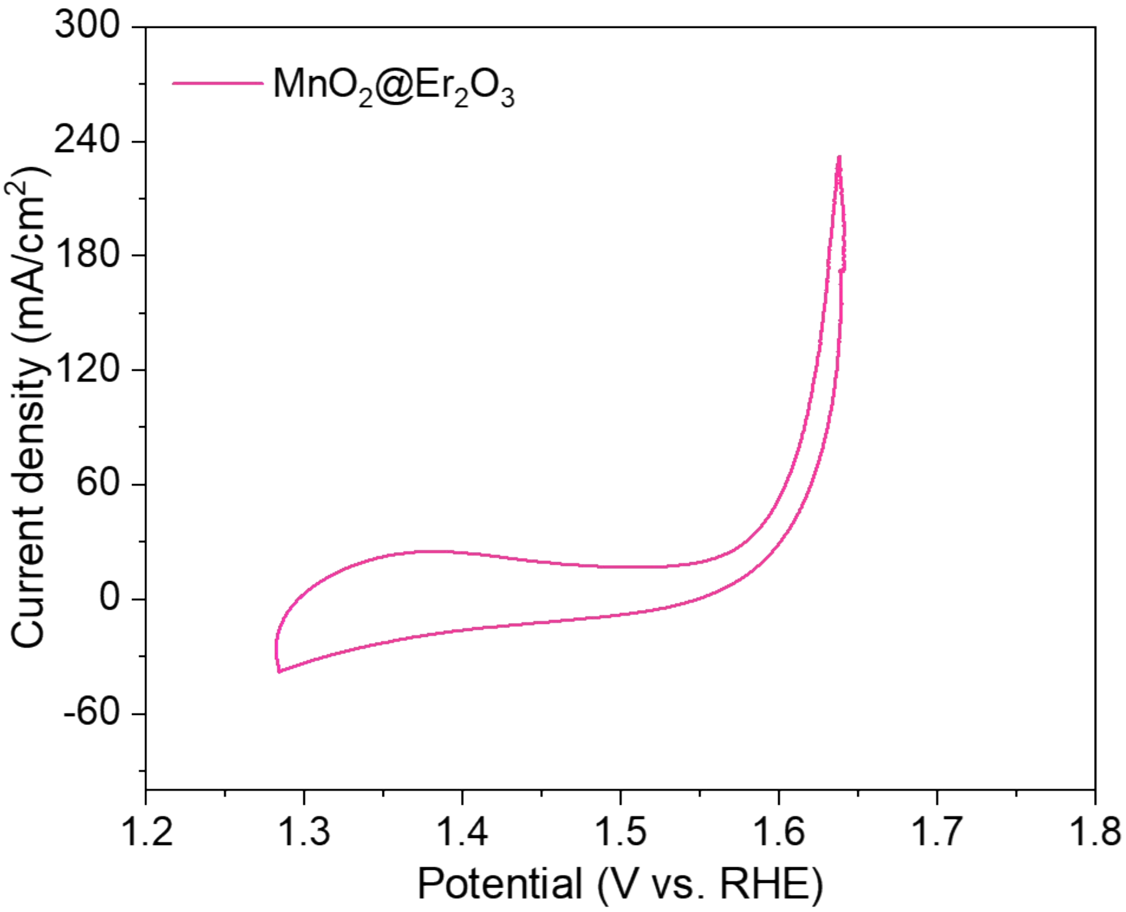

Supplementary Figure 3. Cyclic voltammetry curves of MnO_2@Er_2O_3 (scanning rate: 5 mV/s).

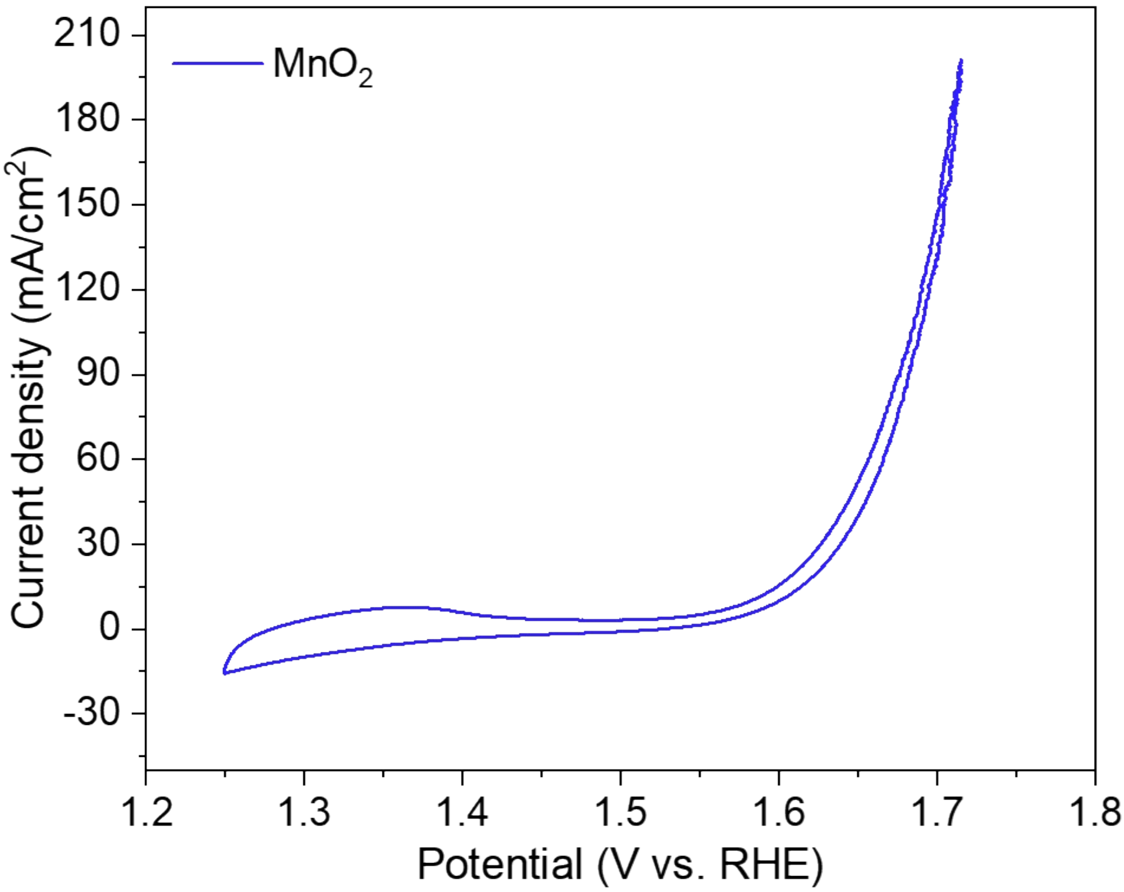

Supplementary Figure 4. Cyclic voltammetry curves of MnO_2 (scanning rate: 5 mV/s).

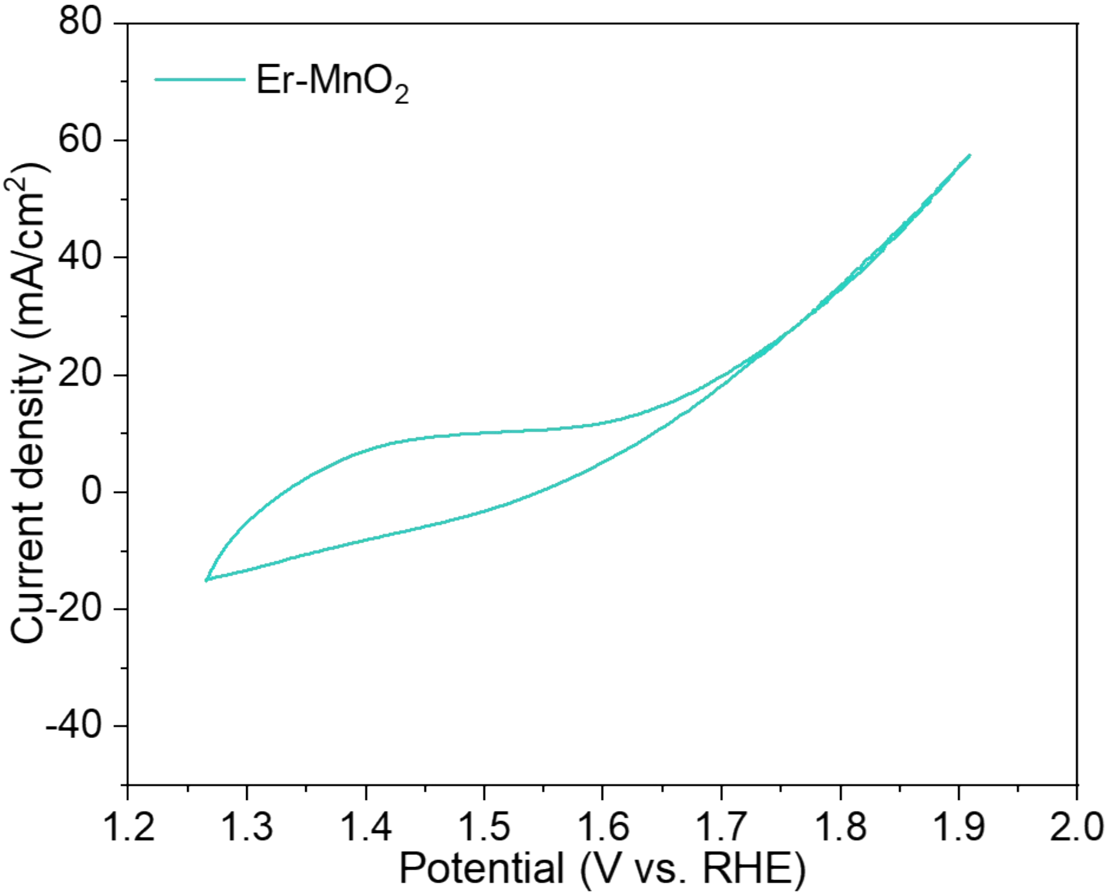

Supplementary Figure 5. Cyclic voltammetry curves of Er-MnO_2 (scanning rate: 5 mV/s).

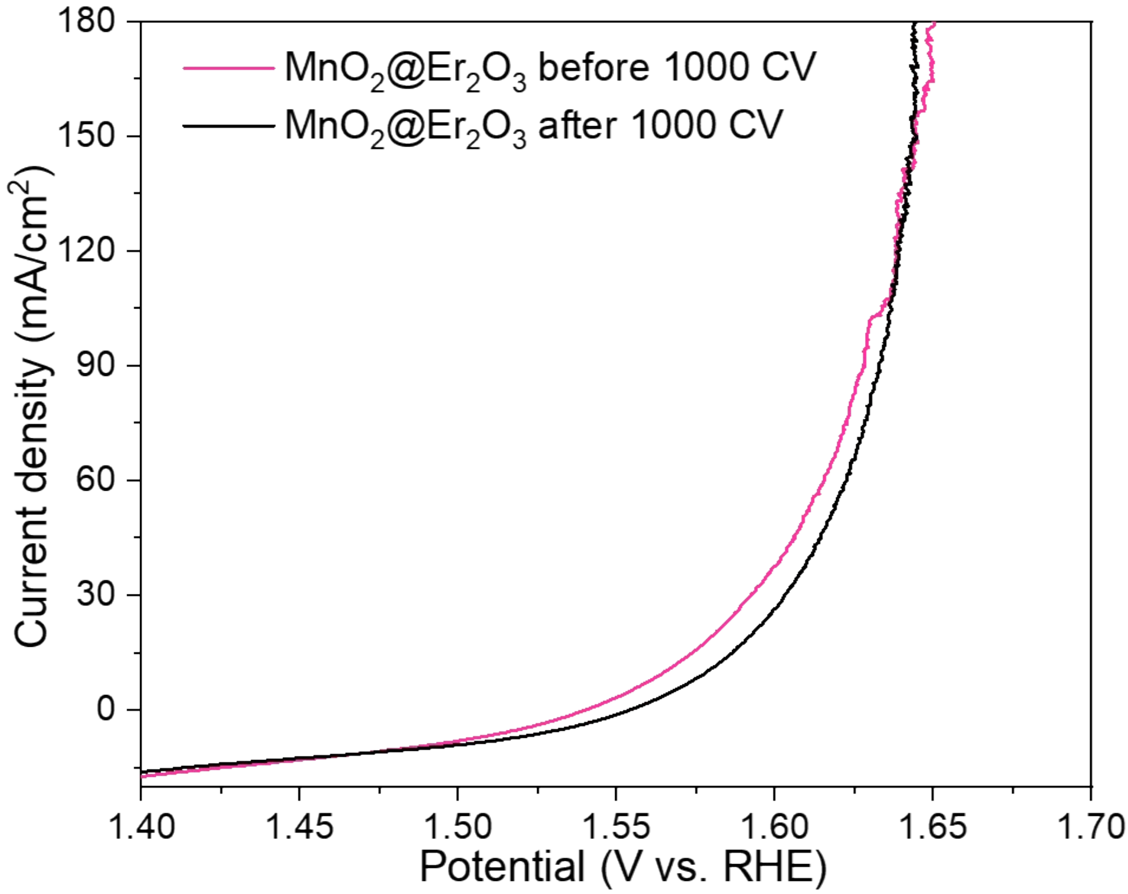

Supplementary Figure 6. Linear sweep voltammograms of the $MnO_2@Er_2O_3$ catalyst before and after 1000 CV cycles.

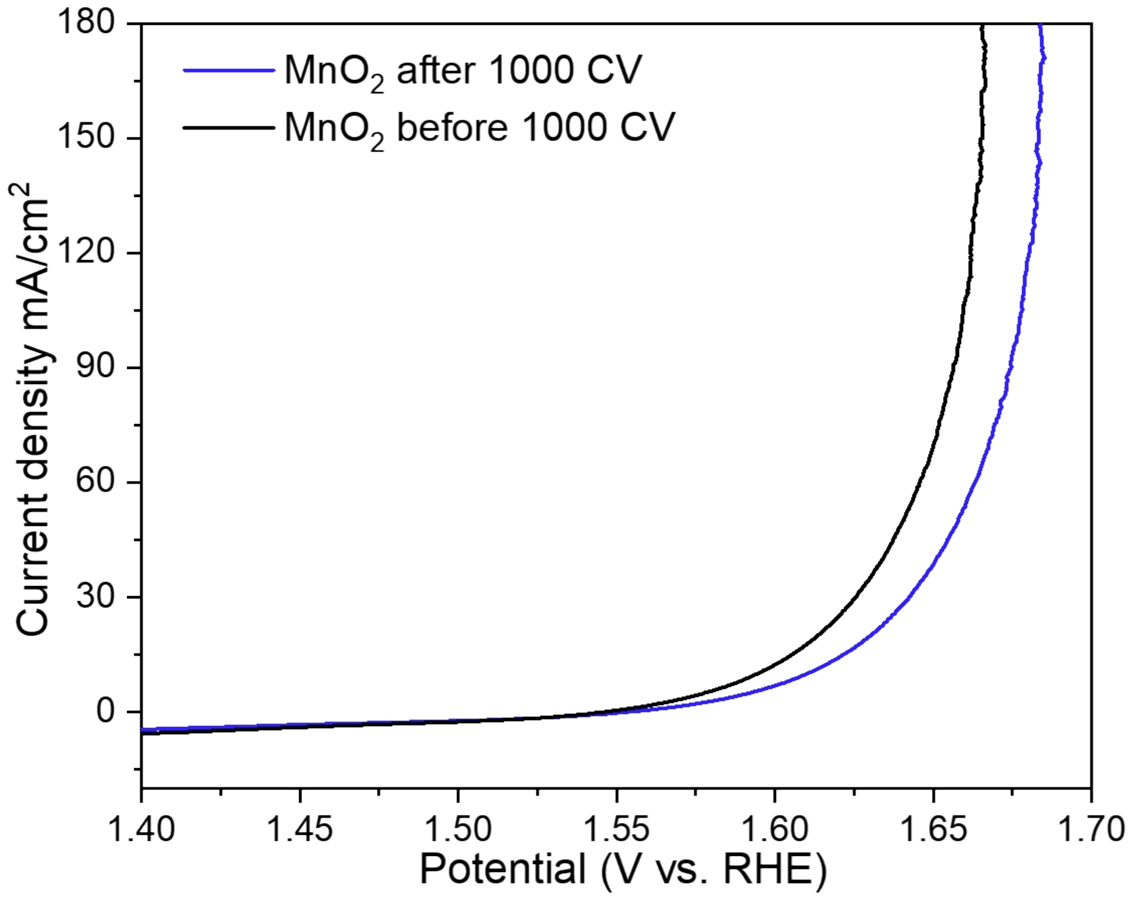

Supplementary Figure 7. Linear sweep voltammograms of the MnO_2 catalyst before and after 1000 CV cycles.

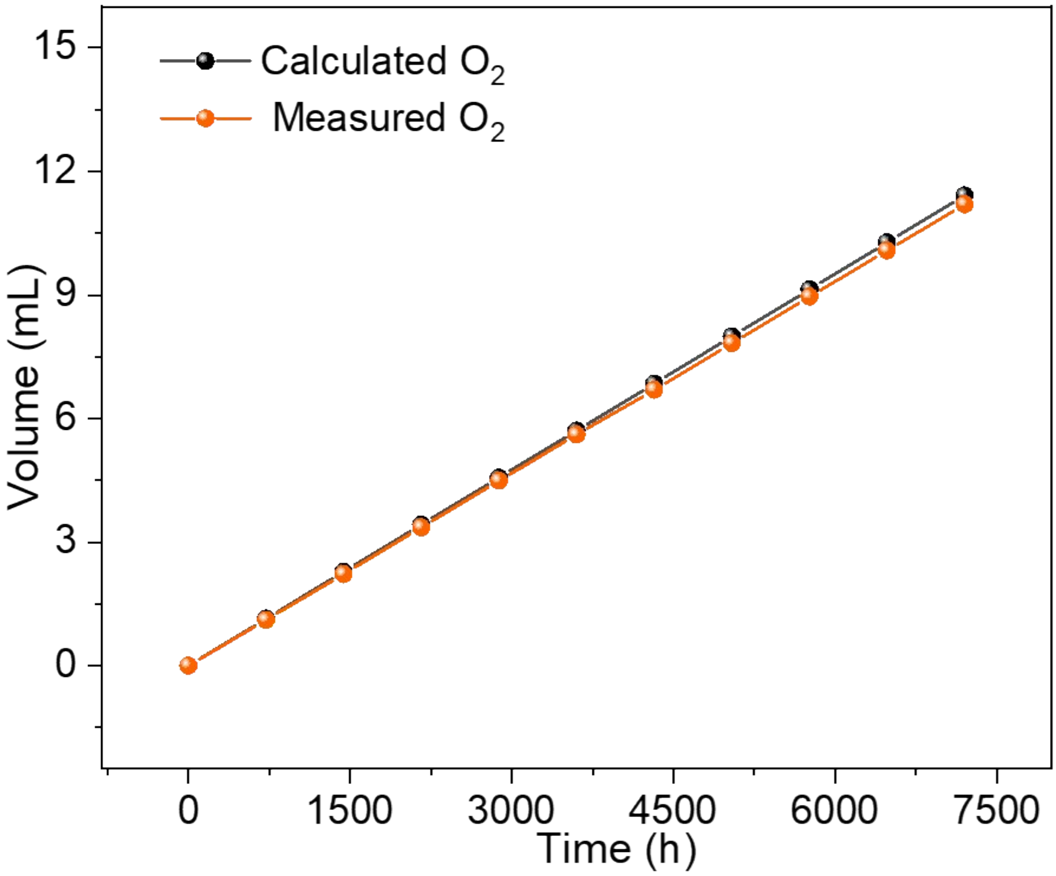

Supplementary Figure 8. Experimental and theoretical volumes of O_2 by the $MnO_2@Er_2O_3$ electrode in a sealed H-type electrolyzer at a current density of 50 mA cm^{-2}.

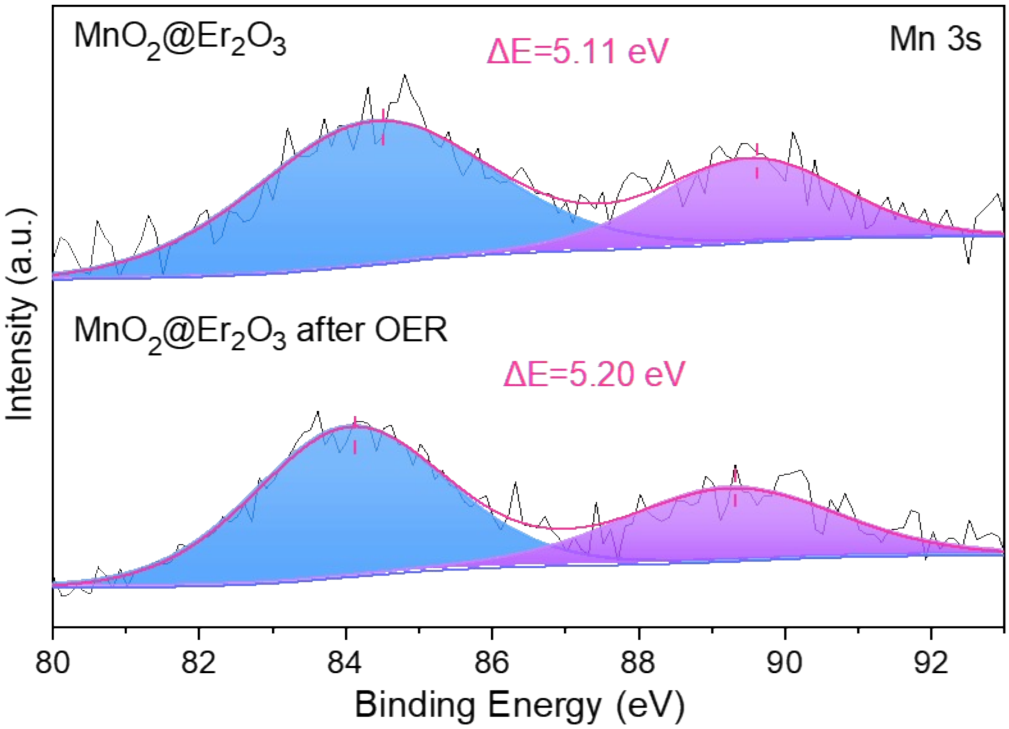

Supplementary Figure 9. The Mn 3s XPS spectra of MnO_2@Er_2O_3 before and after OER reaction.

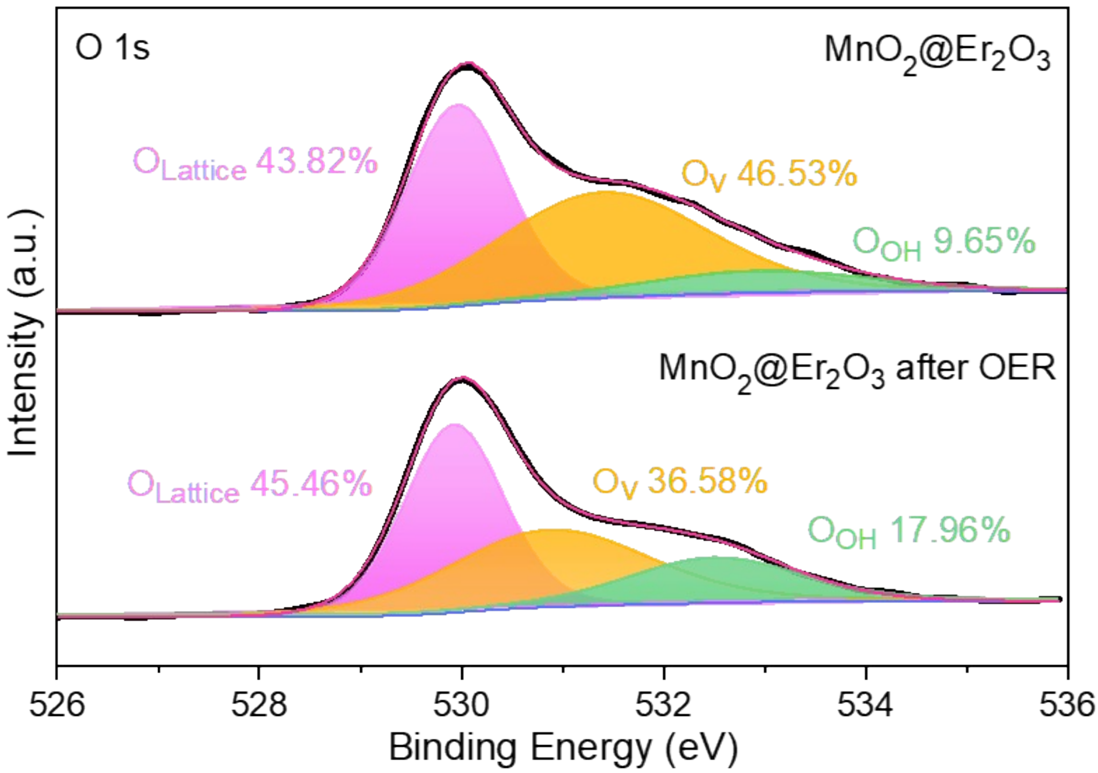

Supplementary Figure 10. The O 1s XPS spectra of MnO_2@Er_2O_3 before and after OER reaction.

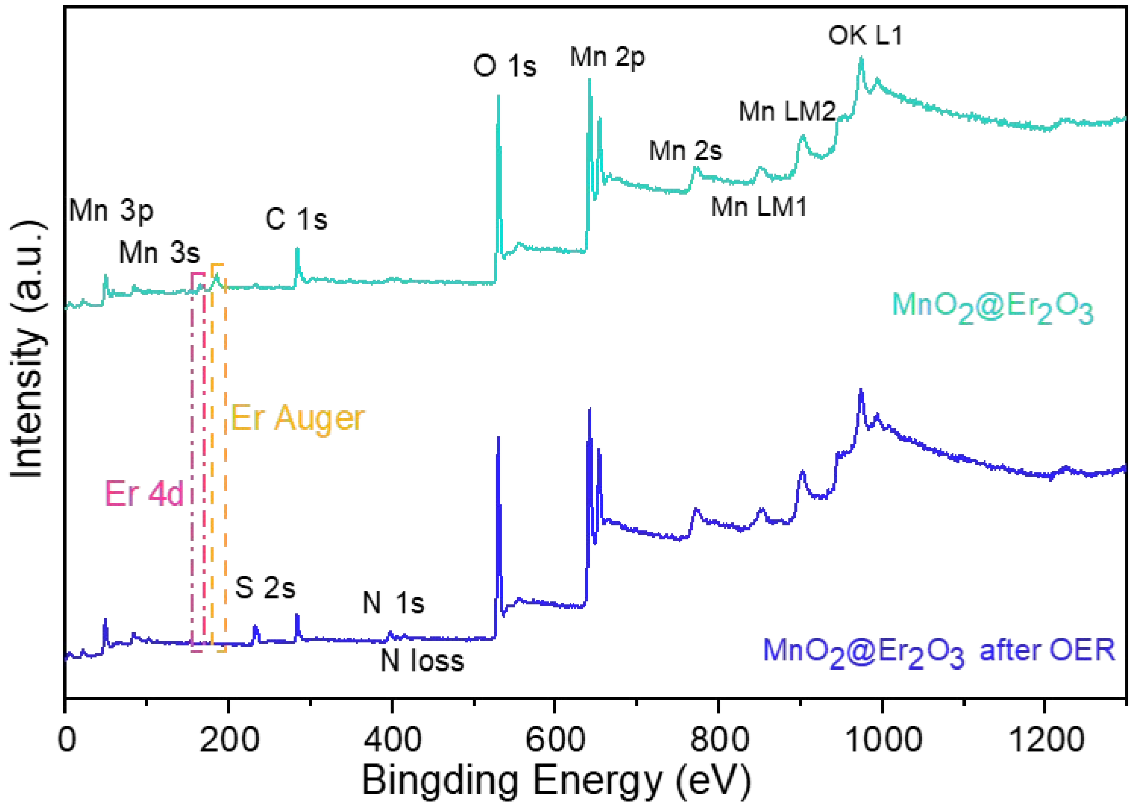

Supplementary Figure 11. The full-survey XPS spectra of $MnO_2@Er_2O_3$ before and after OER.

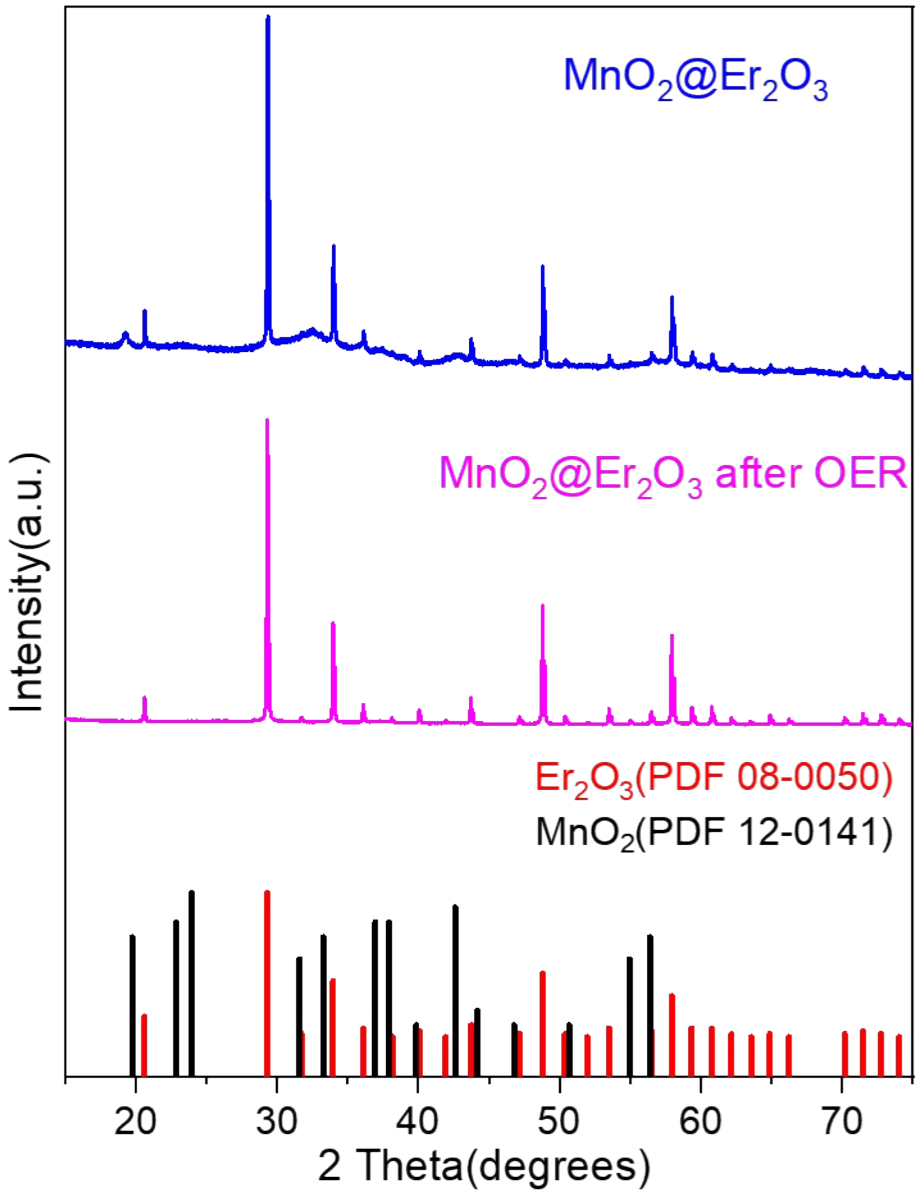

Supplementary Figure 12. XRD patterns of $MnO_2@Er_2O_3$ before and after the OER reaction.

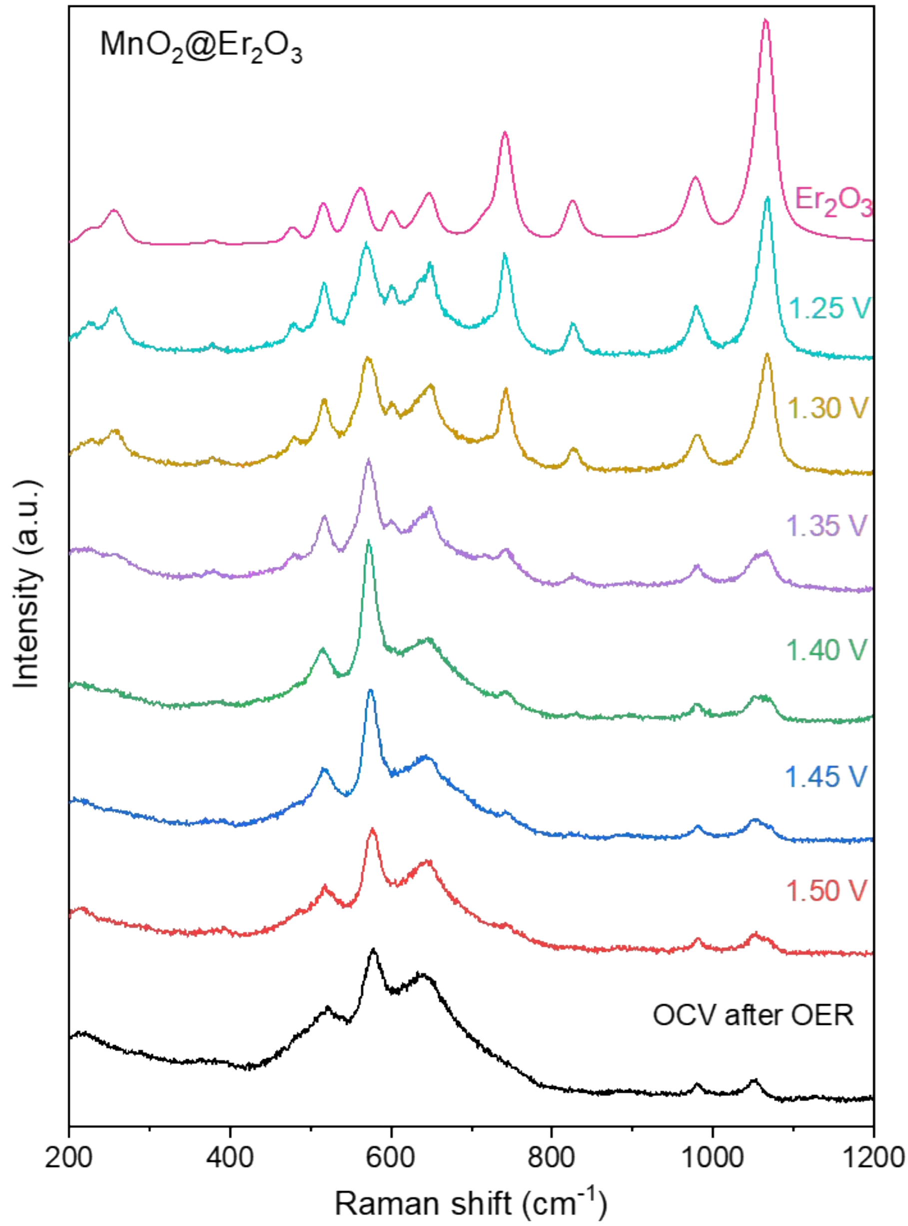

Supplementary Figure 13. In situ Raman spectra of $MnO_2@Er_2O_3$ on a carbon cloth in 0.5 M H_2SO_4 electrolyte under different external applied potentials (0-1.50 V) and the Raman spectra of Er_2O_3.

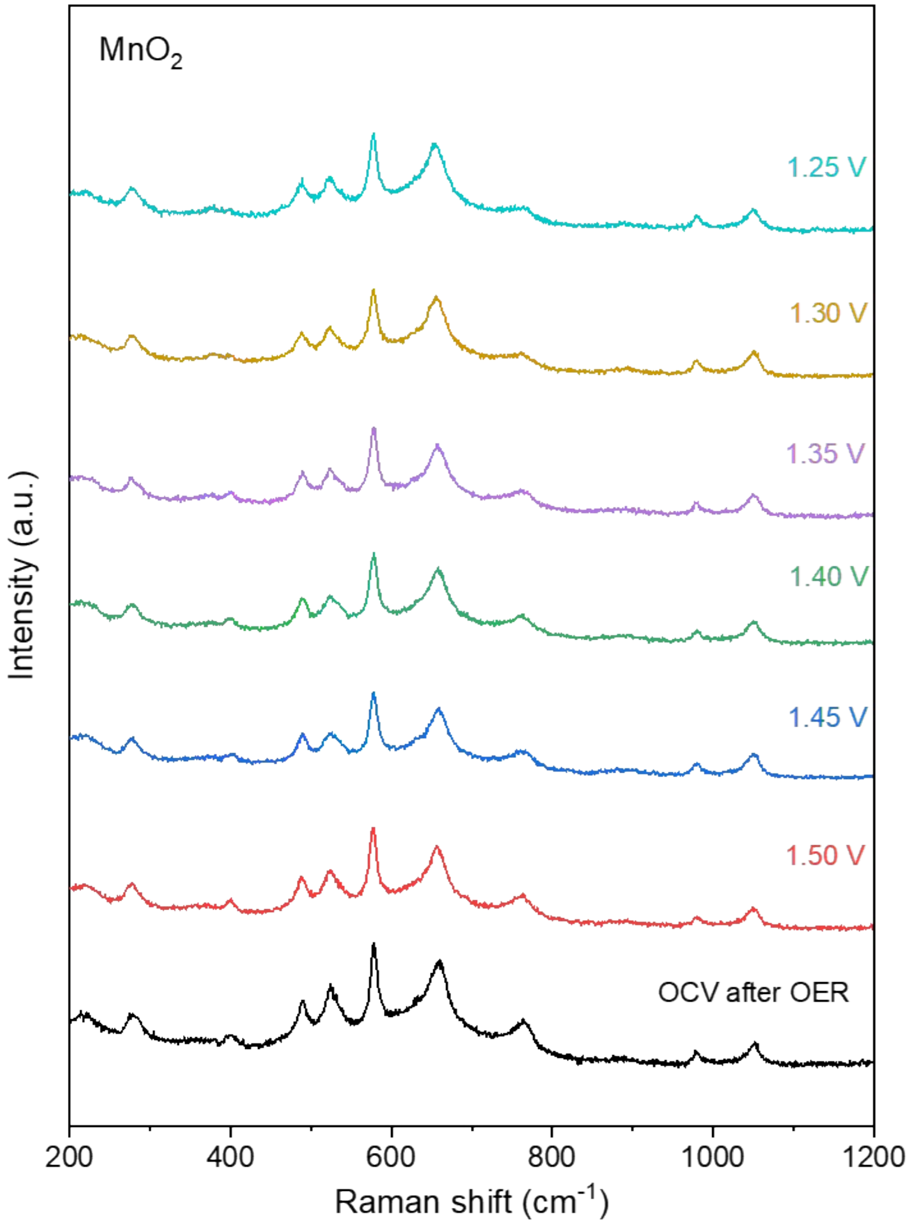

Supplementary Figure 14. In situ Raman spectra of MnO_2 on a carbon cloth in 0.5 M H_2SO_4 electrolyte under different external applied potentials (0-1.50 V).

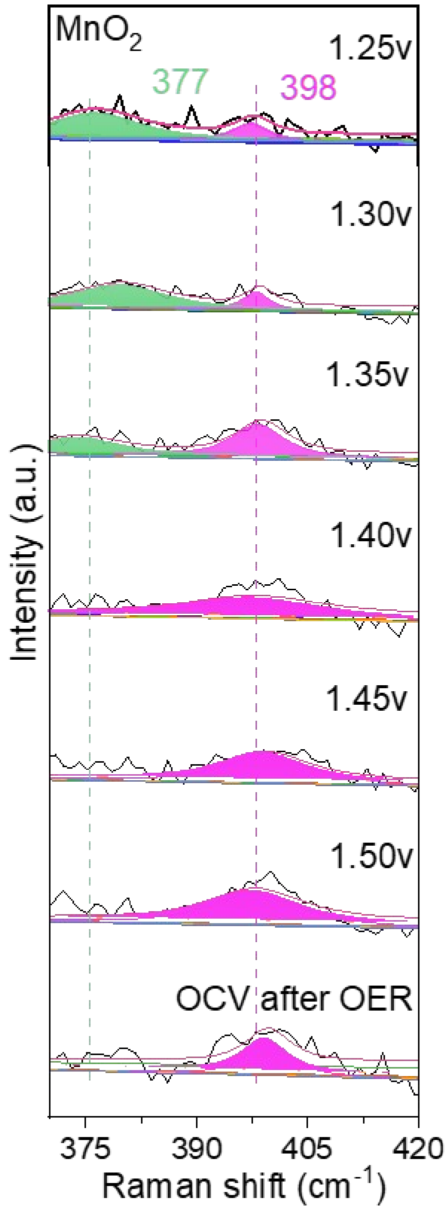

Supplementary Figure 15. Local magnification of in-situ Raman spectra of MnO_2 in 0.5 M H_2SO_4 at different applied potentials (1.25 ~ 1.50 V vs. RHE).

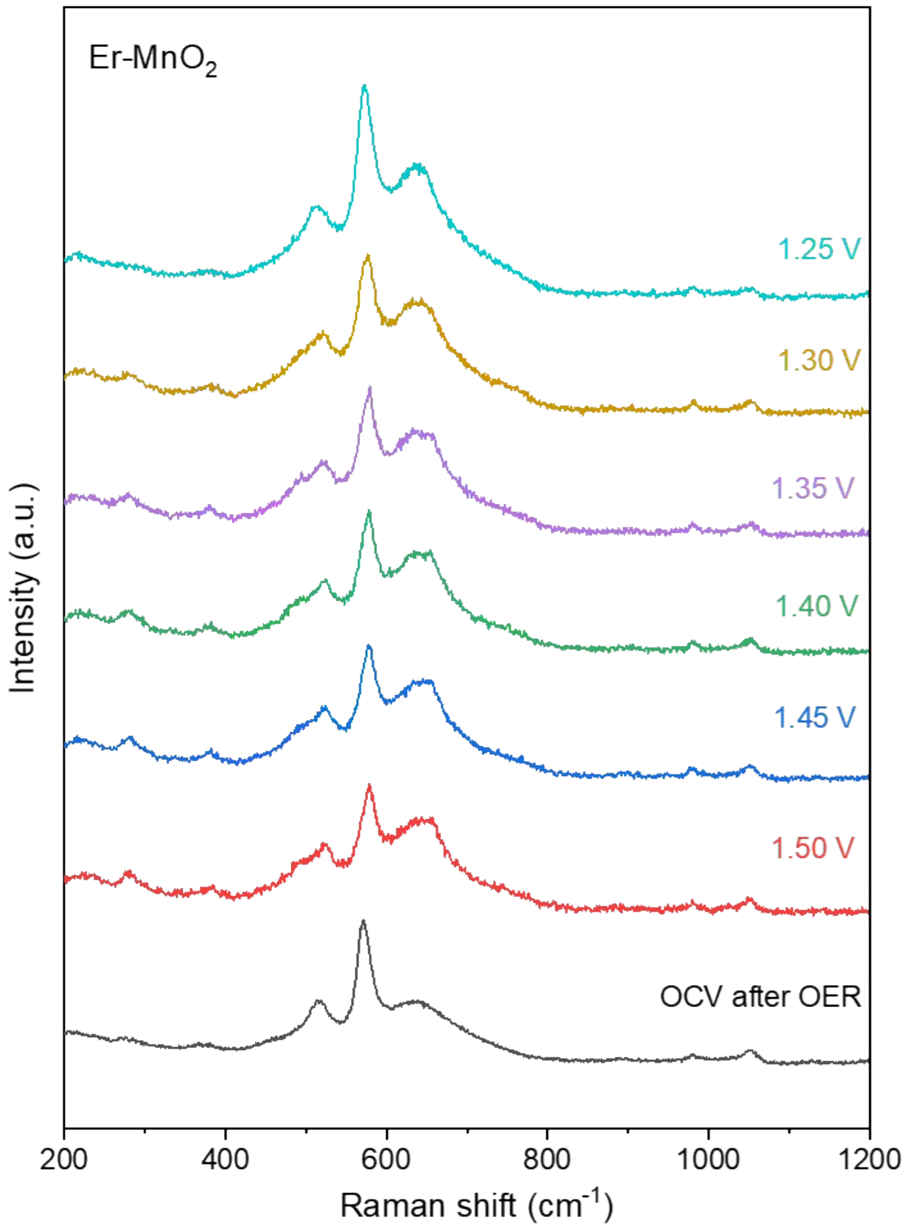

Supplementary Figure 16. In situ Raman spectra of Er-MnO_2 on a carbon cloth in 0.5 M H_2SO_4 electrolyte under different external applied potentials (0-1.50 V).

Supplementary Table 1. Faradaic efficiency of the produced oxygen amount during the water splitting process.

		O_2	
Time (s)	$V_{experimental}$ (mL)	$V_{theoritical}$ (mL)	ŋ/%
0	0	0	0
720	1.11	1.142	97.198
1440	2.22	2.284	97.198
2160	3.36	3.426	98.074
2880	4.49	4.568	98.292
3600	5.61	5.710	98.249
4320	6.70	6.852	97.782
5040	7.83	7.994	97.948
5760	8.96	9.136	98.074
6480	10.08	10.278	98.074
7200	11.20	11.420	98.074

Supplementary Table 2. Calculation of Er element content dissolved in the electrolyte.

Catalyst	The mass of the Er element on the electrode	The mass of the Er element of the electrolyte	The dissolution percentage
MnO_2@Er_2O_3	7.032 mg	1.512 mg	21.5 %

Supplementary Table 3. The chemical bond order of the newly formed bond in the structure is shown in Figure 5c.

<table>
<tr><td></td><td colspan="2">Mn</td><td colspan="2">Er</td></tr>
<tr><td></td><td>8</td><td>18</td><td>22</td><td>23</td></tr>
<tr><td>O_{Mn}10</td><td>0.299965</td><td>0.538043</td><td>0.389292</td><td>1.032118</td></tr>
<tr><td></td><td colspan="2">11</td><td>22</td><td>23</td></tr>
<tr><td>O_{Er}26</td><td colspan="2">0.32661611</td><td>0.269091</td><td>0.383728</td></tr>
<tr><td></td><td colspan="2">20</td><td colspan="2">22</td></tr>
<tr><td>O_{Er}28</td><td colspan="2">2.41607104</td><td colspan="2">0.69405935</td></tr>
<tr><td></td><td>1</td><td>8</td><td colspan="2">23</td></tr>
<tr><td>O_{Er}29</td><td>0.104977</td><td>1.302225</td><td colspan="2">0.62970807</td></tr>
<tr><td></td><td colspan="2">15</td><td colspan="2">21</td></tr>
<tr><td>O_{Er}30</td><td colspan="2">0.76844035</td><td colspan="2">0.38141591</td></tr>
</table>

Supplementary Table 4. The bond level of the relevant Mn-O bond is in Figure 5j.

Mn	O	bond order	Mn	O	bond order
1	2	1.32137312	18	9	0.8387735
	3	1.17778928		10	1.031023
	23	1.42058366		12	1.1375752
5	3	0.99617465		16	0.619006
	6	1.11056846		19	0.8880831
	7	1.05999733	11	4	1.2562912
13	7	1.12815407		10	0.1607694
	14	1.40854525		12	0.9287973
15	14	0.79146615		21	2.0088235
	16	0.70028285	8	2	0.9361188
	17	0.87465018		4	0.9056777
	24	2.07554841		6	0.2699771
20	16	0.83824363		9	0.7096119
	17	1.20796969		10	0.813882
	19	1.17173555			
	22	1.95657879			

Supplementary Table 5. Summary of noble-metal-free OER catalyst performance from this work and previous typical literature.

Catalyst	Electrolyte	η (mV) @ j (mA cm^{-2})	Stability	Ref.
MnO_2@Er_2O_3	**0.5 M H_2SO_4**	**342@10**	**20 h@50 mA cm^{-2}**	**This work**
MnO_2	**0.5 M H_2SO_4**	**406@10**	**11 h@50 mA cm^{-2}**	**This work**
La- and Mn-codoped porous cobalt spinel fibers	0.1 M $HClO_4$	353@10	360 h@10 mA cm^{-2}	*Science. 2023, 380 (6645), 609-616.*
Co_3O_4/FTO	0.5 M H_2SO_4	570@10	50 h@1 mA cm^{-2}	*Chem. Mater. 2017, 29, 950–957.*
$CoMnO_x$	pH = 2.5	540@0.1	8 h@0.1 mA cm^{-2}	*J. Am. Chem. Soc. 2015, 137, 14887–14904.*
Co_3O_4@C/carbon paper	0.5 M H_2SO_4	370@10	86.8 h@10 mA cm^{-2}	*Nano Energy. 2016, 25, 42-50.*
CoFeNiMoWTe	0.5 M H_2SO_4	373@10	100 h@10 mA cm^{-2}	*Adv. Energy Mater. 2023, 13, 2301420.*
Mn-doped FeP/$Co_3(PO_4)_2$	0.5 M H_2SO_4	390@10	8.33 h@5 mA cm^{-2}	*ChemSusChem. 2019, 12, 1334-1341.*
Ba [Co-POM]	1 M H_2SO_4	410@10	24 h@1.48 V vs. RHE	*Nat. Chem. 2018, 10, 24-30.*
Fe-Co_3O_4@C/FTO	0.5 M H_2SO_4	396@10	50 h@10 mA cm^{-2}	*Appl. Catal. B. 2022, 303, 120899.*
$Co_{0.05}Fe_{0.95}O_y$	0.5 M H_2SO_4	650@10	85 h@10 mA cm^{-2}	*Chem. Commun. 2019, 55, 5017-5020.*
CoFePb/Pt-Ti	0.05 M H_2SO_4	620@10	160 h@10 mA cm^{-2}	*Nature Catalysis. 2019, 2 (5), 457-465.*
Co_3O_4/CeO_2 on carbon paper	0.5 M H_2SO_4	347@10	50 h@10 mA cm^{-2}	*Nat Commun. 2021, 12 (1), 3036.*
P-Co_3O_4	0.1 M $HClO_4$	400@10	30 h@10 mA cm^{-2}	*J. Colloid Interface Sci. 2023, 641, 329-337.*
Co_2TiO_4/CC	0.5 M H_2SO_4	513@10	10 h@1.79 V vs. RHE	*Inorg. Chem. 2019, 58, 8570-8576.*
NiCo-nitrides/$NiCo_2O_4$/GF	0.5 M H_2SO_4	460@10	40 h@1.4 V vs. RHE	*Adv. Sci. 2019, 6, 1801829.*
Mo-Co_9S_8@C	0.5 M H_2SO_4	370@10	24 h@10 mA cm^{-2}	*Adv. Energy Mater. 2020, 10, 1903137.*
Co_3O_4/PGC	0.5 M H_2SO_4	510@10	-	*J Energy Chem. 2020, 49, 8-13.*